



UNIVERSIDADE ESTADUAL DE CAMPINAS  
SISTEMA DE BIBLIOTECAS DA UNICAMP  
REPOSITÓRIO DA PRODUÇÃO CIENTÍFICA E INTELLECTUAL DA UNICAMP

**Versão do arquivo anexado / Version of attached file:**

Versão do Editor / Published Version

**Mais informações no site da editora / Further information on publisher's website:**

<https://www.scielo.br/j/bor/a/D65ZbJH6TfKVDC4X7xfSYZr>

**DOI:** <https://doi.org/10.1590/1807-3107bor-2023.vol37.0011>

**Direitos autorais / Publisher's copyright statement:**

©2023 by Sociedade Brasileira de Pesquisa Odontológica. All rights reserved.

DIRETORIA DE TRATAMENTO DA INFORMAÇÃO

Cidade Universitária Zeferino Vaz Barão Geraldo

CEP 13083-970 – Campinas SP

Fone: (19) 3521-6493

<http://www.repositorio.unicamp.br>

# Synchronous jawbone diseases: a multicenter retrospective study

Diogo dos Santos da Mata REZENDE<sup>(a)</sup>   
Lucas Lacerda de SOUZA<sup>(a)</sup>   
Daniel Cavalléro Colares UCHÔA<sup>(a)</sup>   
Lais Albuquerque FERNANDES<sup>(b)</sup>   
Jeanne Gisele Rodrigues de LEMOS<sup>(b)</sup>   
Alan Roger SANTOS-SILVA<sup>(a)</sup>   
Márcio Ajudarte LOPES<sup>(a)</sup>   
Lady Paola Aristizabal ARBOLEDA<sup>(a)</sup>   
André Caroli ROCHA<sup>(c)</sup>   
Fábio Luiz Neves GONÇALVES<sup>(b)</sup>   
Flávia Sirotheau Corrêa PONTES<sup>(b)</sup>   
Felipe Paiva FONSECA<sup>(d)</sup>   
Hélder Antônio Rebelo PONTES<sup>(a)</sup> 

<sup>(a)</sup>Universidade Estadual de Campinas – Unicamp, Piracicaba Dental School, Department of Oral Diagnosis, Piracicaba, SP, Brazil.

<sup>(b)</sup>Universidade Federal do Pará – UFPA, João de Barros Barreto University Hospital, Department of Oral Pathology, Belém, PA, Brazil.

<sup>(c)</sup>Universidade de São Paulo – USP, School of Medicine, Clinics Hospital, Department of Oral and Maxillofacial Surgery, Medical School, São Paulo, SP, Brazil.

<sup>(d)</sup>Universidade Federal de Minas Gerais – UFMG, School of Dentistry, Department of Oral Surgery and Pathology, Belo Horizonte, MG, Brazil.

**Declaration of Interests:** The authors certify that they have no commercial or associative interest that represents a conflict of interest in connection with the manuscript.

**Corresponding Author:**  
Hélder Antônio Rebelo Pontes  
E-mail: harp@ufpa.br

<https://doi.org/10.1590/1807-3107bor-2023.vol37.0011>

Submitted: December 28, 2020  
Accepted for publication: June 2, 2021  
Last revision: November 9, 2021

**Abstract:** The aim of this study is to report an original case series of synchronous jawbone diseases. Data of patients seen over 13 years were extracted from the files of three Oral Radiology and Pathology diagnostic centers in Brazil. The clinical, radiographic, and laboratory characteristics were tabulated and analyzed by the authors; the patients were described according to lesion type. Seventy-two synchronous jawbone diseases were included in this study. Florid osseous dysplasia, Gorlin-Goltz syndrome, and cherubism were the most frequent disorders reported in this case series. In addition, the posterior mandible area was the main site of manifestation. Florid osseous dysplasia and Gorlin-Goltz syndrome represented two-thirds of our samples. With the utilization of adequate demographic, clinical, and radiologic information, it is possible to diagnose most of the synchronous lesions of jawbones. Sometimes, however, we need complementary exams, such as histopathologic and biochemical analysis or dosing of calcium, phosphorus, and alkaline phosphatase.

**Keywords:** Pathology; Mandible; Maxilla; Jaw; Bone and Bones.

## Introduction

Two or more lesions are considered synchronous when they affect more than one site at the same time, or have a maximum of six months difference between diagnoses, and are referred to as metachronous when they occur at separate times (excluding the possibility of recurrence or metastasis).<sup>1,2</sup> The diagnosis of these disorders can represent a challenge for radiologists due to the uncommon occurrence, heterogeneity, similar radiologic features, and the limited clinical and demographic information available about the patient at the time of imaging.<sup>3</sup> Image exams can show a range of bone alterations including osteolytic, sclerotic, or mixed conditions in appearance.<sup>4</sup>

Synchronous jaw disorders have been rarely described in the literature and limited to the specific lesions. Therefore, we describe a case series of synchronous jawbone diseases (SJB), emphasizing the importance of correlating the parameters of images with clinical, demographic, and in some cases, with histological and biochemical analysis to achieve the correct diagnosis.



## Methodology

All cases in which patients had synchronous jawbone manifestations were retrospectively retrieved from the files from the Oral Medicine, Oral Pathology, and Oral and Maxillofacial Surgery Departments of the João de Barros Barreto University Hospital (Belém, Brazil), Piracicaba Dental School of the University of Campinas (Piracicaba, Brazil), and Clinics Hospital of the Medical School of the University of São Paulo (São Paulo, Brazil) from January 2007 to December 2019. The data included sex, age, signs and symptoms, as well as the oral and maxillofacial affected sites. The available image findings of panoramic radiograph (PR), computed tomography (CT), or magnetic resonance imaging (MRI) were registered. In addition, biochemical analysis and histopathological/immunohistochemical information were assessed for final diagnosis.

Apical periodontitis lesions, periodontitis, and disorders with inconclusive diagnosis were excluded. This study followed the guidelines proposed in the Helsinki Declaration and was approved by the local Institutional Ethical Committee.

## Results

Over 13 years, 120 SJBD cases were identified at the study centers. A total of 48 cases were excluded because they represented inflammatory diseases, resulting in 72 case reports. The clinical and radiographic characteristics of each disorder included are summarized in Table 1. The most frequent diseases were florid cemento-osseous dysplasia (FCOD) (33 cases; 45.8%), Gorlin-Goltz syndrome (GGS) (11 cases; 15.2%), and cherubism (6 cases; 8.3%). The lesions were more prevalent in females, with a male:female ratio of 1:2. The mean age of the patients was 37.6 years (range: 5–84 years).

FCOD was identified in 33 cases, representing 45.8% of all cases. The mean age was 51 years (range: 11–84). This group demonstrated a higher prevalence in female patients, with a male:female ratio of 1:32. The main diagnostic criteria were clinical exam (CE), PR, and CT (21 cases; 63.3%). Under radiographic evaluation, the most common

image was well-defined and dense radiopacities surrounded by radiolucent rims was demonstrated (23 cases, 69%). The patients were more affected in two quadrants for this disease (20 cases; 60.6%). The second most prevalent disease was GGS, with 11 cases (15.2%). The mean age was 23 years (range: 8–74). The male:female ratio was 8:3, demonstrating a higher prevalence in male patients. The lesions' diagnostic criteria included CE and PR in all 11 cases, and a clinical exam, PR, and CT in 6 cases (54.5%). The most observed radiographic aspects were well defined, unilocular, radiolucent image (eight cases; 72.7%). The lesion showed mainly two affected quadrants (9 cases; 81.8%) followed by four affected quadrants (3; 27.2%).

Cherubism was found in 6 cases (8.3%). Cherubism did not demonstrate any sex predominance, with a male:female ratio of 1:1 and a mean age of 14.6 years (range: 5–36). The main diagnostic criteria for this lesion were CE and PR (6 cases; 100%). Radiographically, all lesions were presented as multilocular radiolucencies (6 cases; 100%). Four quadrants were affected for this syndrome in 5 cases (83.4%). Brown tumor of hyperparathyroidism (BTH) corresponded to four cases (5.5%). BTH demonstrated a strong predominance for males (4 cases; 100%) at a mean age of 53 years (range: 29–64). CE, RP, CT, laboratory examination (LE), and biopsy were performed for diagnosis in all four cases. The most observed radiographic aspect was multiple radiolucencies (4 cases; 100%). BTH showed two affected quadrants in two cases and three quadrants in two cases.

Multiple myeloma was observed in four cases (5.5%). They were mainly seen in male patients with a mean age of 65 years old (range 54–84 years old). Diagnostic criteria was based on CE, PR, CT and biopsy in all cases. Radiographic aspects showed radiolucent multilocular lesions in all analyzed patients. MM evidenced four affected quadrants in four cases and two quadrants in two cases. Simple bone cyst (SBC) were found in three cases (4.1%). SBC was observed mainly in male patients (2 cases; 66.6%) and in one case, the sex was not reported; the mean age was 15 years (range: 13–19). In two cases, the diagnostic criteria were CE, PR, and CT (66.6%). The radiographic aspect was mainly a well-defined,

**Table 1.** Clinicopathological and radiographic characteristics of the synchronous jaw lesions analyzed in the present study. n(%)

Lesions	Patients	Sex	Mean age (range)	Radiographic aspects	Diagnostic criteria	Affected quadrants
Florid cemento-osseous dysplasia	33 (45.8)	32 F (96.9)	51 (11–84)	23 (69)	21 (63.3)	2 Affected = 20 (60,6)
		1 M (3.03)		Well-Defined, Dense Radiopacities Surrounded by Radiolucent Rims.	Clinical Examination, Panoramic Radiograph, Computed Tomography	3 Affected = 5 (15.1)
						4 Affected = 7 (21,2)
Gorlin-Goltz syndrome	11 (15.2)	3 F (27.2)	23 (8–74)	8 (72.7)	6 (54.5)	2 Affected = 9 (81,8)
		8 M (72.7)		Well-Defined, Unilocular, Radiolucent Image	Clinical Examination, Panoramic Radiograph, Computed Tomography	4 Affected = 3 (27,2)
Cherubism	6 (8.3)	3 F (50)	14.6 (5–36)	6 (100)	6 Cases (100)	2 Affected = 5 (83,4)
		3 M (50)		Multilocular Radiolucencies	Clinical Examination, Panoramic Radiograph	4 Affected = 1 (16,6)
						1 (16,6)
Brown tumor of hyperparathyroidism	4 (5.5)	4 M (100)	53 (29–64)	4 (100)	4 Cases (100)	2 Affected = 2 (50)
				Multiple Radiolucencies	Clinical Examination, Panoramic Radiograph, Computed Tomography, Laboratory Examination, Biopsy	3 Affected = 1 (25)
						4 Affected = 1 (25)
Multiple Myeloma	4 (5.5)	3 M (75)	65 (54–84)	4 (100)	Clinical examination, Panoramic radiographic, Computed tomography,	4 affected = 2 (50)
		1 F (25)		Multilocular, Radiolucent, Multilocular or Mixed	Biopsy	2 affected = 2 (50)
Simple bone cyst	3 (4.1)	2 M (66.6)	15 (13–19)	2 (66.6)	2 (66.6)	
		1 NR (33.3)		Well-Defined, Unilocular, Radiolucent Image	Clinical Examination, Panoramic Radiograph, Computed Tomography	2 Affected = 3 (100)
				1 (33.3)	1 (33.3)	
				Ill-Defined, Unilocular, Dense Radiopaque Surrounded By Radiolucent Image	Clinical Examination, Panoramic Radiograph	

Continue

Continuation						
Dentigerous cysts	2 (2.7)	2 M (100)	8.5 (05–12)	2 (100) Well-Defined, Unilocular, Radiolucent Image	2 (100) Clinical Examination, Panoramic Radiograph	2 Affected = 2 (100)
Langerhans cell histiocytosis	2 (2.7)	2 M (100)	14.5 (11–18)	2 (100) Ill-Defined, Radiolucent Image	2 (100) Clinical Examination, Panoramic Radiograph, Biopsy	4 Affected 2 (100%)
Paget's disease	2 (2.7)	1 F (50)	49 (48–58)	2 (100)	2 (100)	2 Affected = 1 (50)
		1 M (50)		Cotton-wool Like Radiopacity	Clinical Examination, Panoramic Radiograph Computed Tomography, Laboratory Examination	4 Affected = 1 (50)
Gardner syndrome	2 (2.7)	2 F (100)	15.5 (13–18)	1 Case (50) Well-Defined, Unilocular, Dense Radiopacities	1 Case (50) Clinical Examination, Panoramic Radiograph	2 Affected = 1 (50)
				1 (50) Ill-Defined, Multilocular, Radiolucent Image	1 (50) Clinical Examination, Panoramic Radiograph, Computed Tomography	4 Affected = 1 (50)
Ossifying fibroma	1 (1.38)	F	21 (-)	Well-Defined, Unilocular, Radiolucent Image	Clinical Examination, Panoramic Radiograph, Computed Tomography, Laboratory Examination, Biopsy	2 Affected
Osteitis fibrosa cystica	1 (1.38)	M	27 (-)	Multiple Radiolucencies	Clinical Examination, Panoramic Radiograph, Computed Tomography, Laboratory Examination, Biopsy	4 Affected
Idiopathic Osteosclerosis	1 (1.38)	M	74 (-)	Generalized irregular radiopacity	Clinical Examination, Panoramic radiographic	4 Affected

F, Female; M, Male; NR, not reported.

unilocular, radiolucent image (two cases; 66.6 %). All cases had two affected quadrants.

Dentigerous cysts (DC) were seen in 2 cases (2.7%), both being male at a mean age of 8.5 years (range: 5–12). Radiographically, all cases presented were well-defined, unilocular, radiolucent images associated with the crowns of an unerupted permanent tooth, and the diagnostic criteria were CE and PR (two cases; 100%). The two cases had two affected quadrants. Langerhans cell histiocytosis (LCH) corresponded to 2 cases (2.7) in males at a mean age of 14.5 years (range: 11–18). Under the main diagnostic criteria, CE, PR, and biopsy were performed in both cases (100%) and both cases presented an ill-defined, radiolucent image, and had four affected quadrants.

Paget's disease (PD) were found in 2 cases (2.7%, one man, one woman, at a mean age of 49 years [range: 48–58]). The main diagnostic criteria were CE, PR,

CT, and LC. When radiographically evaluated, all lesions showed cotton wool-like radiopacity. One case presented four affected quadrants, and the other case presented two quadrants that were affected. Gardner syndrome (GS) occurred in 2 cases in women (2.7%) at mean age 15.5 years (range: 13–18). In 1 case, the diagnostic criteria were CE and PR, and in the other, the criteria were CE, PR, and CT. Radiographically, the images presented well-defined, unilocular, and dense radiopacities in one of the cases and an ill-defined, multilocular, radiolucent image in the other. Considering the affected quadrants, 1 case presented four affected quadrants (50%) and 1 case presented 2 affected quadrants (50%).

Central ossifying fibroma (OF) represented 1.38% (one case) of our sample: a 21-year-old woman, who underwent CE, PR, CT, LE, and biopsy. The radiographic aspect was a well-defined, unilocular,

radiolucent image, and two mandibular quadrants were affected. Osteitis fibrosa cystica (OFC) was found in one case (1.38%), a 27-years-old man. Radiographs showed multiple radiolucencies and the diagnostic criteria were CE, PR, CT, LE, and biopsy; four quadrants were affected. Idiopathic osteosclerosis was observed in one case (1.38%) in a 74-year-old male patient. PR showed a generalized irregular radiopacity. Diagnosis was based on CE and PR, and lesion affected four quadrants of the patient.

## Discussion

To the best of our knowledge, this is the first case series study with different types of synchronic jawbone diseases. It is well known that the diagnosis of SJBD must follow a holistic approach that combines demographic, biochemical, clinical, and radiologic information. The method proposed by us is to focus on image features with the other necessary data to complete the diagnosis of each disease shown in Table 2.

According to our study, the most prevalent SJBD was FCOD, representing almost 50% of all cases. This condition occurs above the inferior alveolar canal, surrounding the root apices or in edentulous areas.<sup>5</sup> The process is confined to an alveolar process, including interdental and interradicular septa. Subsequently, the newly formed bone spreads to the periodontal space without compromising pulp vitality and radicular reabsorption or changes in dental position (Figure 1A).<sup>6</sup> FCOD has a symmetrical pattern, affecting at least two and, in many cases, even four quadrants. In the early immature osteolytic stage, the radiographic features are entirely radiolucent with a round or ovoid configuration, mimicking an inflammatory periapical lesion. The intermediate stage is characterized by a mixed radiolucent and radiopaque appearance (cotton wool appearance). In the final stage, the lesion becomes a densely mineralized mass (radiopaque), usually with a radiolucent rim.<sup>7</sup> When an SBC is associated with FOCD, multilocular radiolucency can be detected and may result in an expanded or perforated cortical bone, as seen in three cases in the present series.<sup>5</sup> The FOCD diagnosis can be achieved by PR.<sup>8</sup> CT and

cone-beam computed tomography (CBCT) should be performed in lesions in the maxilla due to the greater difficulty of diagnosis. Kato et al.<sup>9</sup> showed that on CT examination, FOCDs can present with the cortical bone intact, slight thinning, expansion, and is less frequently perforated. In addition, the mandible is always involved, especially in posterior areas, as observed in this study.

The OF image has an oval shape, generally unilocular, with corticated margins and without root resorption, and according to the degree of calcification, completely radiolucent or as mixed images (Figure 1B).<sup>10</sup> Expansion without perforation of cortical bone and displacement of teeth are associated with larger lesions.<sup>11</sup> Synchronous OF tends to occur in the mandible and maxilla, with one lesion in each area. Simultaneous lesions in the mandible, as seen in our work, are unusual. It is noteworthy that synchronous OF can be a manifestation of hyperparathyroidism.<sup>12</sup>

PD presents, in general, in polyostotic form involving many skeletal bones, with jawbones being involved in 15% of cases (Figure 2A-C).<sup>13</sup> The upper jaw is more affected than the lower jaw. In the early phase (osteolytic phase), radiolucent areas predominate (ground glass appearance), leading to the loss of the lamina dura when the lesion involves migration and resorption of the roots of teeth. In the osteoblastic phase, the radiopacity spreads in most of the areas, leading to the enlargement of the jaws, with alveolar ridges become widened (cotton wool appearance). The focal loss of lamina dura and hypercementosis allows the differentiation of PD from hyperparathyroidism.<sup>14</sup> Bone scintigraphy (Figure 2D-H) is recommended to delineate the alteration of mandible bone (Lincoln's sign).<sup>13</sup>

Osteopetrosis is an inherited metabolic bone disorder with a clinical spectrum ranging from mild to severe that shows uniform and generalized sclerosis of the skeleton due to a failure in bone resorption (impaired osteoclast activity or development). Parallel bands of dense bone in the vertebrae and long bones give the impression of 'bone-within-bone'. The condition causes obliteration of medullary spaces, especially in long bones, skull (macrocephaly, frontal bossing), and spine, with increased bony trabeculae and thickened cortices (Figure 3D).<sup>15</sup>

**Table 2.** Definitions, etiology, clinical features, and biochemical analysis of the synchronous jawbone lesions.

Disease	Definition	Etiology	Signs and symptoms	Age group	Sex/Race	Other comorbidities	Biochemical analysis
Florid osseous dysplasia	Reactive or dysplastic process characterized by the substitution of normal bone by fibrous connective tissue, with subsequent immature bone deposition that gradually becomes sclerotic.	Unknown	Asymptomatic or painful swelling in edentulous areas, with bone exposure or after extractions.	Fifth to sixth decades of life.	Female/Black people.	Not reported.	Not reported.
Central ossifying fibroma	Benign neoplasm, which arises from mesenchymal blast cells of the periodontal ligament.	Unknown	Asymptomatic	Second and third decades of life.	Female/No predilection.	Hyperparathyroidism Association	Not reported.
Paget's disease	Polyostotic metabolic disorder caused by osteoclast dysfunction leading to an altered bone remodeling.	Mutation in the SQSTM-1 gene	Pain in the affected bones during all course of the disease.	After the fifth decade of life, rare before the age 40.	Male/White people.	Facial paralysis and deafness associated with due to the narrowing of skull foramina. Sacrum, pelvis, skull and femur are the most affected bones.	Elevated alkaline phosphatase.
Nevoid basal-cell carcinoma syndrome	Autosomal dominant inheritable condition.	Mutation in the Patched gene	Asymptomatic	First and second decade of life.	No predilection/No predilection.	Multiple nevoid basal-cell carcinomas and palmar or plantar pits. Abnormalities in vertebrae (fused or bifid) and ribs (fused, bifid, splayed or missing) and calcification of cerebral falx. Frontal and temporoparietal bossing, prominent supra-orbital ridges and increased occipitofrontal circumference.	Not reported.
Cherubism	Autosomal dominant genetic condition which giant cell lesions replace the bone.	Mutation in SH3BP2 gene (80% of cases).	Painful lesions due to nerves compression.	First decade of life.	Males slightly more affected/No predilection.	Lymph node involvement.	Elevated alkaline phosphatase
Brown tumor of hyperparathyroidism	Disorder caused by elevated levels of parathyroid hormone.	Tumor in parathyroid gland or advanced chronic kidney disease	Painful or asymptomatic lesions.	Fourth decade of life	No predilection/No predilection.	Lesion in the parathyroid gland and/or advanced chronic kidney disease.	Hypophosphatemia, elevated levels of serum calcium and parathyroid hormone.
Simple bone cyst	Empty or fluid-filled cavity that develops within bone.	Unknown.	Asymptomatic.	Second decade of life.	Female/No predilection.	Not reported.	Not reported.

Continue

Continuation

Dentigerous cyst	Cyst associated with the crowns of permanent teeth.	Unknown	Asymptomatic	First and second decades of life.	No predilection/ No predilection	Association with cleidocranial dysplasia, basal cell naevus syndrome or mucopolysaccharidosis type IV.	Not reported.
Osteopetrosis	Genetic disorder presents the normal bone formation but reduced bone resorption resulting in the excessive calcified tissue	Mutations in the TCIRG1, SNX10, OSTM1, PLEKHM, TNFSF11 TNFRSF11A and CLCN7 genes.	Bone fracture.	Severe infantile or malignant type: At birth or at the first months of infancy.		Severe infantile or malignant type: anemia hepatomegaly, splenomegaly, lymphadenopathy, blindness, hydrocephalus, exophthalmos, small thorax and hypertelorism and problems during tooth eruption.	Low serum Ca <sup>2+</sup> levels associated with secondary hyperparathyroidism; carbonic anhydrase 2 deficiency in the osteopetrosis with renal tubular acidosis and cerebral calcification form; levels of alkaline phosphatase, 1,25-dihydroxyvitamin D3 and lactate dehydrogenase vary from patient to patient and are (unreliable as biomarkers for the disease); elevated levels of lactate dehydrogenase, aspartate aminotransferase, correlate with autosomal dominant.
				Osteopetrosis with renal tubular acidosis and cerebral calcifications: Early childhood.	No predilection/ No predilection.	Osteopetrosis with renal tubular acidosis and cerebral calcifications: short stature and mental retardation.	
				Intermediate type osteopetrosis: children and adults.		Benign osteopetrosis or Albers-Schönberg disease: Without symptoms.	
Langerhans cell histiocytosis	Abnormal proliferation of bone marrow-derived histiocytes (Langerhans cells) which comprise an unusual group of disorders with focal or systemic manifestations.	Unknown	Pain and mucosa overlying of the gingival and of the hard-palate presents ulcerated	Predominantly seen in children, particularly during early infancy	Slight predominance in man.	Cervical lymphadenopathies. Skull and femoral lesions in children younger than age 10, patients older than age 20 lesions in the ribs, shoulder girdle, and mandible. Seborrheic dermatitis or eczematous eruption on the scalp and trunk. Hepatomegaly Splenomegaly.	Not reported

Continue

Continuation

Multiple myeloma	Cancer of plasma cells, a type of white blood cell that normally produces antibodies.	Unknown.	Swelling and pain.	Older than 60 years.	Man is more affected.	The lesion is commonly associated with anemia, impaired kidney function, infection and neurological symptoms.	Multiple myeloma can produce all classes of immunoglobulin, but IgG paraproteins are most common. Light and or heavy chains (the building blocks of antibodies) may be secreted in isolation: $\kappa$ - or $\lambda$ -light chains or any of the five types of heavy chains ( $\alpha$ -, $\gamma$ -, $\delta$ -, $\epsilon$ - or $\mu$ -heavy chains).
Osteitis fibrosa cystica	A skeletal disorder resulting in replacement of bone to fibrous tissue and the formation of cyst-like brown tumors in and around the bone.	Hyperparathyroidism	Bone pain or tenderness, bone fractures and skeletal deformities.	Before age 40.	No sex predilection.	Weight loss, appetite loss, vomiting, polyuria, and polydipsia.	High levels of calcium, parathyroid hormone and alkaline phosphatase.
Idiopathic Osteosclerosis	A reaction to past trauma or infection.	Unknown.	Focal radiodensity of the jaw which is not inflammatory, dysplastic, neoplastic or a manifestation of a systemic disease.	Teens and those in their 20s	No sex predilection.	None.	None.

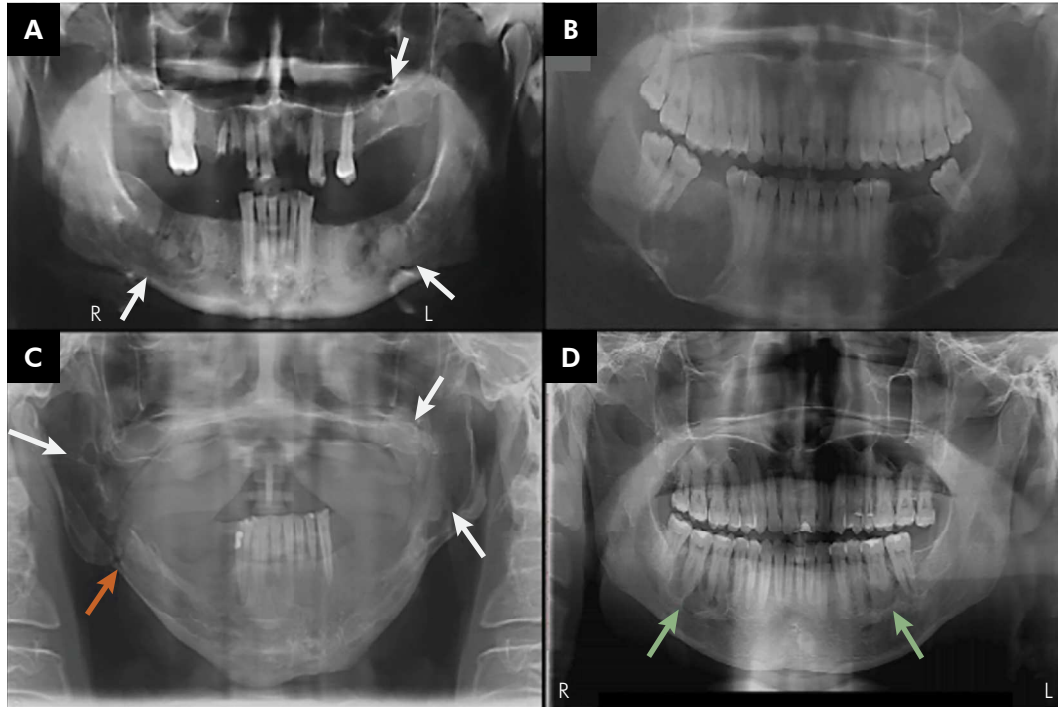


**Figure 1.** (A) Panoramic radiograph of two ossifying fibromas. Well-delimited unilocular, primarily radiolucent lesion containing diffuse calcifications can be seen bilaterally in the mandibular body and downward bowing of the inferior cortex of the mandible on the right side. (B) Mixed density lesions (arrows) consistent with florid osseous dysplasia. Note that the epicenter of the mandibular lesions is above the inferior alveolar canal. (C) Radiographic findings observed in a patient diagnosed as Gorlin-Goltz syndrome demonstrating multiple well-defined radiolucent images in the posterior areas of the maxilla and mandible (white arrows), and a pathological mandibular fracture was also observed (yellow arrow). (D) Well-defined, radiolucent images (green arrows) extending from the roots of teeth 18-20 and the roots of teeth 30-31, diagnosed as brown tumor of hyperparathyroidism secondary to chronic kidney disease.

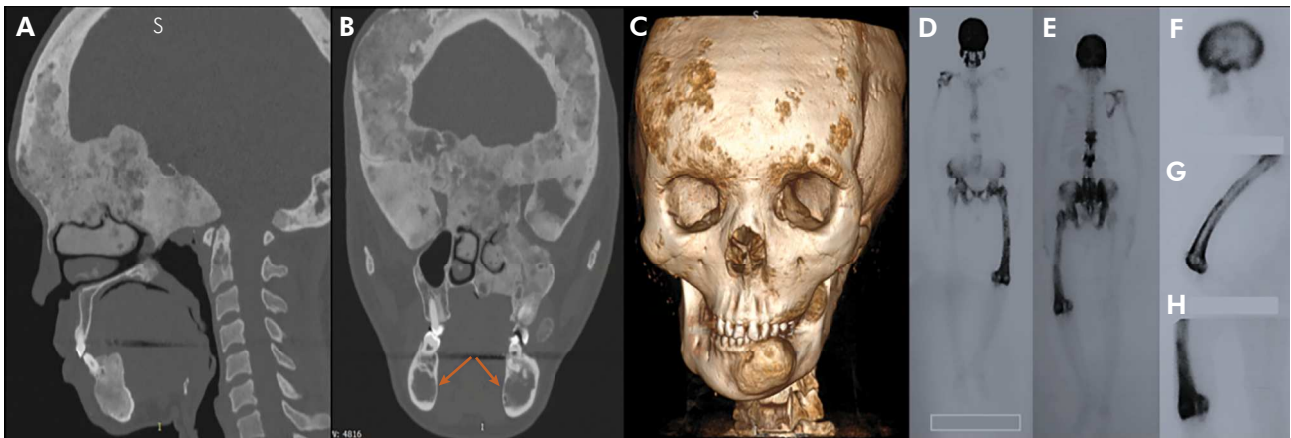


**Figure 2.** (A-D) Computed tomography (CT) of a patient with Gorlin-Goltz syndrome. (A) CT volume rendering-3D image of the thorax showing multiple bifid ribs (green arrows) and scoliosis (blue arrow). (B) Multiple odontogenic keratocysts (white arrows) and calcification in the interhemispheric falx (yellow arrow) on the coronal section. (C) The sagittal section shows significant calcification of the cerebral falx. (D) Sagittal CT demonstrating the diffusely increased density of cranial bones; the ‘stone bone’ aspect that is typically observed in the osteopetrosis. We also observed in parietal and occipital bones a ‘sunburst’ radiographic appearance. (E-F) Odontogenic keratocyst in a patient with Gorlin-Goltz syndrome was presented under histopathological exam a basal layer of the epithelium with columnar cells, presenting a palisade morphology and hyperchromatic nuclei. The capsule of the lesion is formed of loose connective tissue, with ectasic blood vessels and moderate mononuclear inflammatory infiltrate. The most superficial layer of the epithelium with corrugated keratin is shown ((H&E, 50X and 100X).

The condition in jawbones leads to micrognathia. Another important sign seen in our cases was a thickening of the lamina dura as an early sign and an alteration in the medullar bone, which masks the roots.<sup>16</sup> Delayed tooth eruption, tooth agenesis, enamel hypoplasia, and osteomyelitis of the jaws after surgical procedure are common findings.<sup>17</sup>

Multiple odontogenic keratocysts (MOK) are one of the main clinical features of nevoid basal-cell carcinoma syndrome (NBCCS) or GGS. MOK occurs in 75% to 90% of patients with NBCCS. The most common radiographic characteristics are multiple well-defined, unilocular radiolucencies, and the lower jaw is more affected than the upper jaw (Figure 1C).<sup>3,18</sup> Abnormalities in vertebrae

(fused or bifid) and ribs (fused, bifid, splayed, or missing) can be found, and calcification of falx cerebri is pathognomonic (Figure 3A). Also, there is frontal and temporoparietal bossing, prominent supra-orbital ridges, and increased occipitofrontal circumference (Figures 3B, 3C). It is noteworthy that the syndrome is associated with benign neoplasia and other comorbidities. For this reason, it is vital to establish an early diagnosis, for which it is important to keep in mind that MOKs represent the first sign of the syndrome in 75% of patients.<sup>19</sup>

By definition, DC is always associated with the crown of an unerupted permanent tooth at the cemento-enamel junction, and almost all cases of synchronous DC described are associated with third

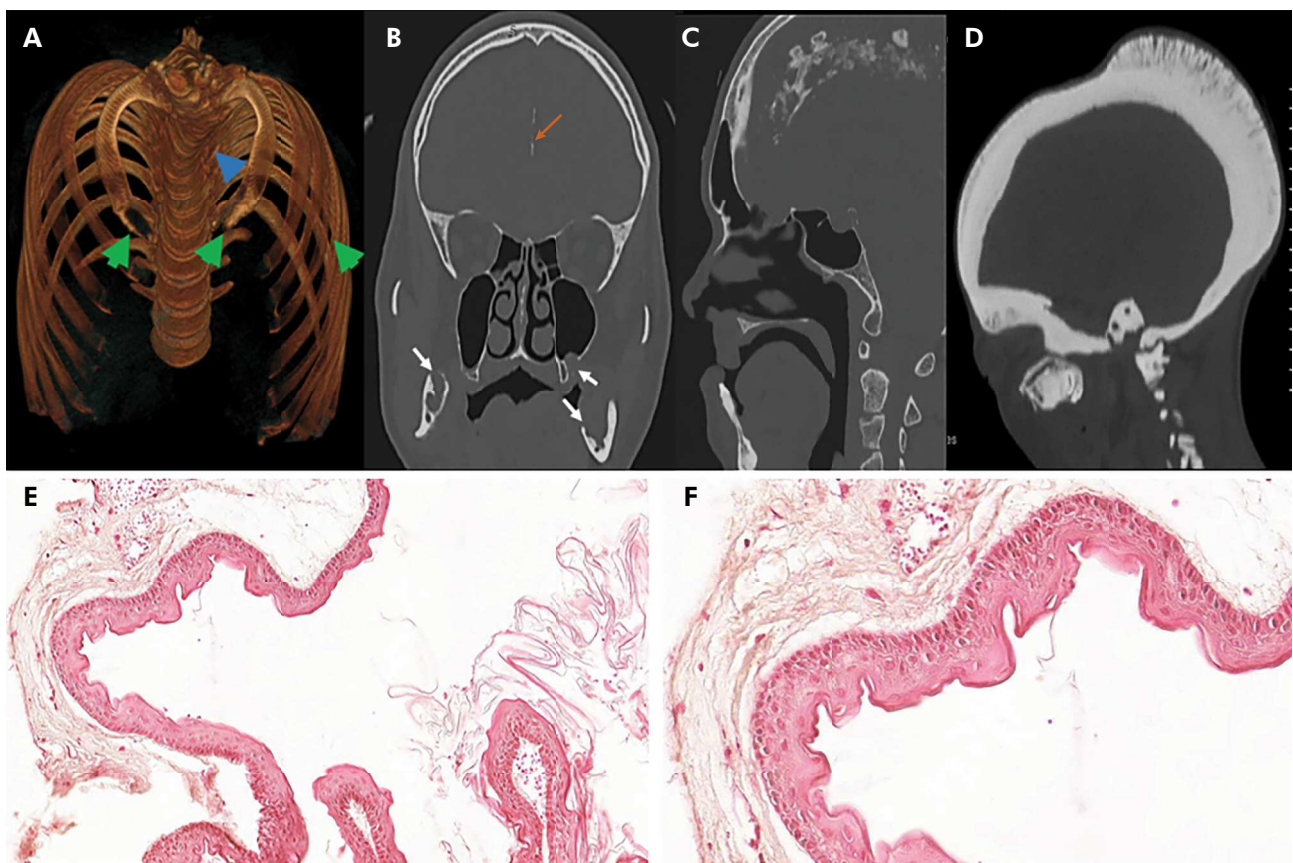


**Figure 3.** Patient with Paget disease. (A) Sagittal and (B) coronal CT images reveal widening and osteosclerosis involving skull and jaws bones. Complete obliteration of frontal, maxillary, and sphenoid sinuses, and also involving middle nasal turbinates. (B) Bilateral lytic areas involving the mandibular bone (yellow arrows). (C) 3D CT volume rendering characterized by areas of bone expansion and distortion, which leads to deformities. (D-H) Total body bone scintigraphy with <sup>99m</sup>Tc showing increased activity and uptake of the radiotracer detected in the skullcap (E), thoracic and lumbar spine (D-E), in the left pelvis (D-E), and femur bones (G-H). Skull (F) and femur in detail are shown (G-H).

molars.<sup>20</sup> Radiographically, DC shows a unilocular radiolucent lesion of corticated borders of more than 5 mm. Synchronous DCs are rare, often associated with cleidocranial dysplasia, basal cell nevus syndrome, or type IV mucopolysaccharidosis.<sup>21,22</sup> In general, DCs are diagnosed in routine radiographic examination or while investigating an asymptomatic swelling. A pathological exam is fundamental for the correct diagnosis, because other cysts, like keratocysts, can mimic the image appearance of DC. MRI provides correct detail on the lesion contents helping in the identification of cyst fluid, with hypodense image on T1 and hyperdense on T2-weighted images.<sup>22</sup>

The face of children affected by cherubism resembles that of cherubs from the Renaissance due to expansion of the cortical bone and consequent swelling of the cheek. Although there are reports of a unilateral manifestation, these cases are not fully accepted as cherubism by the entire scientific community.<sup>23</sup> Under radiographic evaluation, the images have a radiolucent, multilocular aspect and well-defined borders (soap bubble appearance) located in the posterior regions of the mandible

more often than the maxilla. The anterior regions and the adjacent bones can also be affected in the most severe cases of the disease. Bone alterations start in the angle and ascending ramus, expanding from to the mandibular body. Complete obliteration of the sinus is expected in more aggressive cases, and involvement of the orbital cavity can occur (Figure 4A-B). In the mandible, the body, corpus, and angle are affected, with preservation of condylar regions.<sup>24</sup> Tooth displacement, root resorption, or agenesis are common features. Tooth agenesis is associated with more advanced disease.<sup>23,25</sup> CT is the gold standard for evaluating bone lesions of the jaws (Figure 4C-D). In our sample, the condition had an equal prevalence in men and women, and the four quadrants were equally affected.

BTH represents the third most common endocrine disorder after diabetes mellitus and thyroid disease.<sup>26</sup> Radiographically, the condition presents as a multiple hypodense image or as a multiple well-defined, uni or multilocular radiolucency resembling soap bubbles, with the cortical bone expanded (ground-glass appearance) (Figure 1D).<sup>27</sup> Untreated secondary hyperparathyroidism can

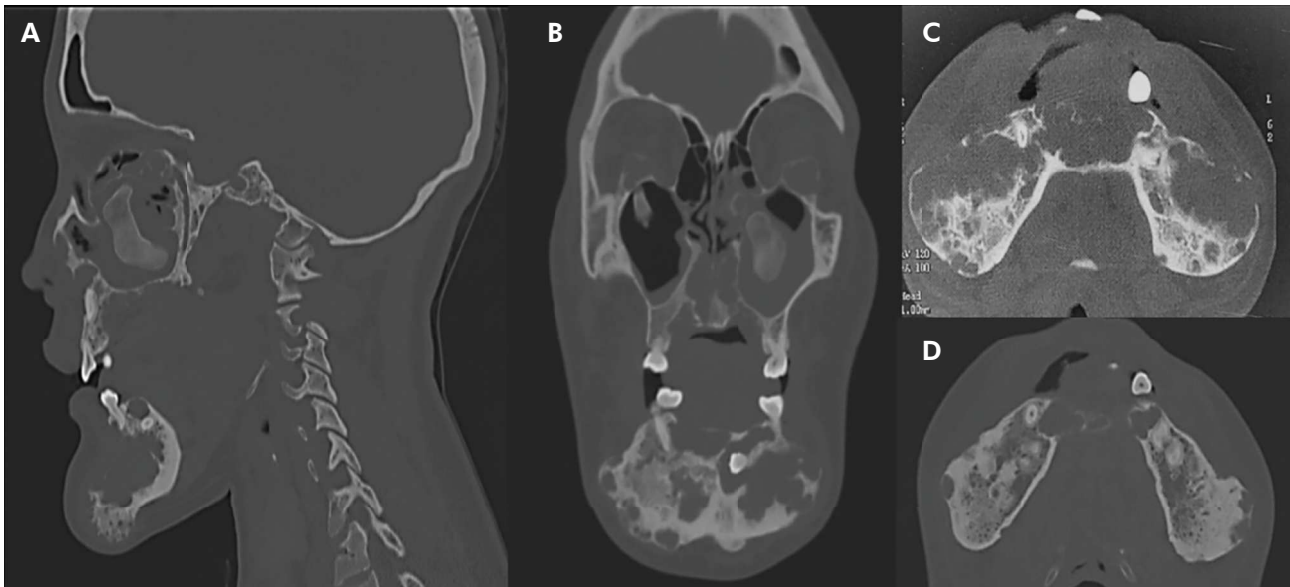


**Figure 4.** CT findings observed in a patient diagnosed as cherubism. Sagittal (A) and coronal (B) images showing multiple bilateral osteolytic lesions located in both jaws and infiltration of the orbital cavities. Partial obliteration of left maxillary sinus. Tomographic changes during the case: at the beginning (C) the lesions are hypodense and later (D), appeared more mineralized. Axial CT image showing significant bilateral distension of the mandibular body (C and D).

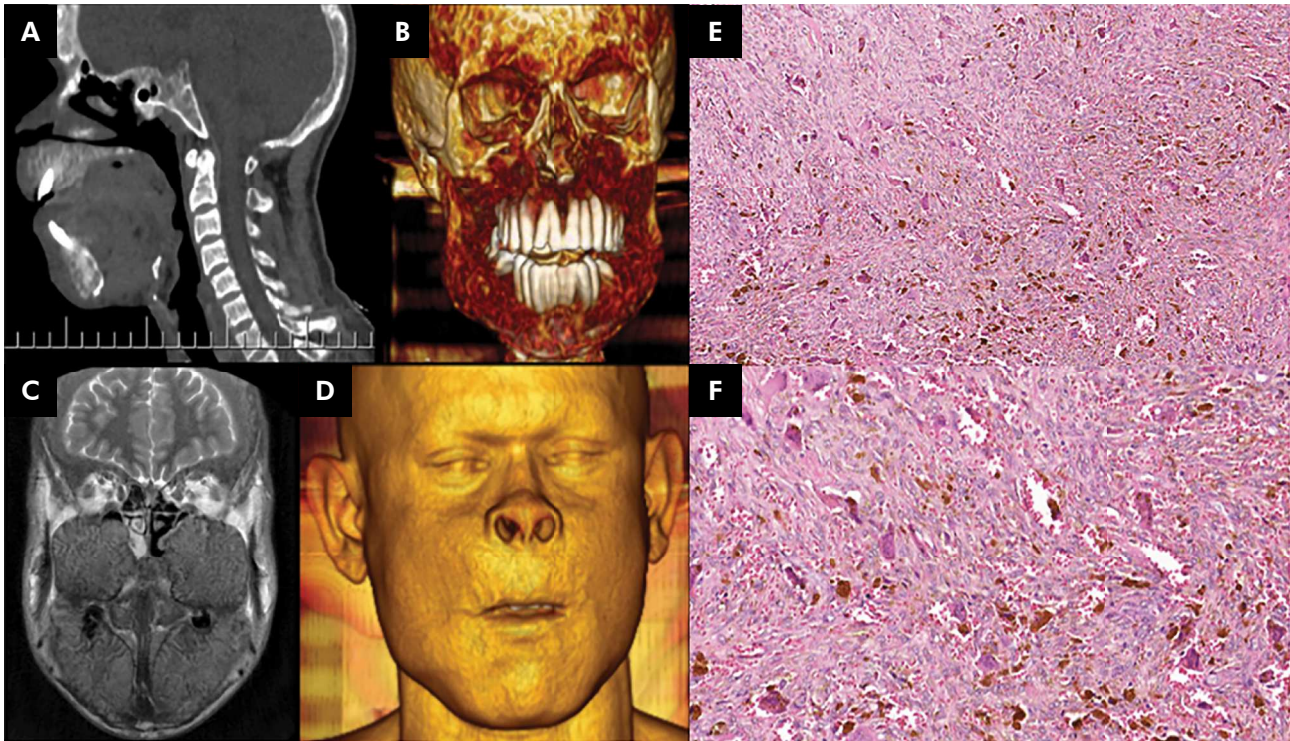


**Figure 5.** Alteration caused by osteitis fibrosa/renal osteodystrophy. (A) Sagittal CT shows poorly delimited hyperdense lesion, with a ‘ground-glass’ appearance in both jaws, sphenoid, frontal, and occipital bones, displaying overgrowth of the maxillary and mandibular bone. The distinct overgrowth of the maxillary bone was profoundly affected by diffuse bone abnormalities (B) which could be illustrated with 3D reconstruction. Other facial and cranial bones were affected. (C) T2 coronal magnetic resonance image demonstrating variable-intensity signals, especially high-intensity signals, in both jaws and maxillary sinus, which was a consequence of the heterogeneous nature of lesions. (D) 3D CT volume rendering depicting leontiasis ossea patient appearance. (E-F) Microscopic aspect of osteitis fibrosa/renal osteodystrophy showing a dense cellular lesion consisting of mesenchymal and multinucleated giant cells, with erythrocytes extravasation (H&E, 50X and 100X).

progress to renal osteodystrophy (RO), which can cause alterations in jawbones in the form of renal osteitis fibrosa (OFi). RO is present in 90% of patients undergoing dialysis.<sup>28</sup> In PR, OFi shows a diffuse ill-defined ground glass appearance with poor corticomedullary distinction and expansion of the cortical bone (Figure 5). The early radiographic appearance of jawbone involvement in OFi are thinning of the cortices and loss of the lamina dura.<sup>29</sup> Root reabsorption and obliteration of the inferior alveolar canal are commonly found.<sup>30</sup>

SBC can occur in association with FOCD, and SBC can manifest synchronously in jawbones. An et al.<sup>31</sup> and Chrcanovic and Gomez<sup>32</sup>, in a systematic review on synchronous SBC, showed that most lesions were located in the posterior mandibular region (mandibular body) and had been diagnosed

in routine radiographic analysis (asymptomatic lesions). Interradicular scalloping is a characteristic. In addition, the authors determined that the most usual radiographic appearance in multifocal SBC was a unilocular shape with well-demarcated borders. The expansion of bone without perforation is more frequent in synchronous lesions than in solitary disease.<sup>32</sup> Moreover, root resorption and the absence of lamina dura can occur.<sup>33</sup>

Langerhans cell histiocytosis (LCH) is a disorder characterized by abnormal proliferation of bone marrow-derived histiocytes. The condition can present focal or systemic manifestations. In jawbones, LCH manifests as solitary or multiple radiolucent circumscribed lesions affecting the alveolar or cortical bone, causing the appearance of floating teeth with disease evaluation. The overlying mucosa is ulcerated,

with gingival inflammation. Bleeding, necrosis, recession, dental mobility, and premature loss of teeth are common occurrences. In many cases, the diagnosis is established through oral lesions.<sup>34</sup>

A significant number of synchronous lesions in association or not with syndromes are described in the literature. Aristizabal Arboleda and collaborators<sup>35</sup> published a case of a 15-year-old female patient who was diagnosed with a calcifying odontogenic cyst associated with dentigerous cyst in the right maxillary sinus. In addition, Só et al.<sup>36</sup> reported a case series of synchronous calcifying epithelial odontogenic tumor of the mandible and maxilla. Moreover, Shao and colleagues<sup>37</sup> also reported the occurrence of odontogenic myxoma with multiple

keratocyst odontogenic in the nevoid basal cell carcinoma syndrome. Interestingly, the presence of synchronous lesions with different histological types were not found in our study.

In conclusion, FOCD, GGS, cherubism, and BTH were the most frequent disorders associated with synchronous jaw lesions in this case series. Also, the posterior mandible area was the main site of manifestation. The utilization of adequate demographic, clinical, and radiologic information allows the appropriate diagnosis of most synchronous jawbone lesions. Sometimes, however, we also need a histopathology exam and biochemical analysis of calcium, phosphorus, and alkaline phosphatase.

## References

1. Panosetti E, Luboinski B, Mamelle G, Richard JM. Multiple synchronous and metachronous cancers of the upper aerodigestive tract: a nine-year study. *Laryngoscope*. 1989 Dec;99(12):1267-73. <https://doi.org/10.1288/00005537-198912000-00011>
2. Zhang Q, Li Y, Gao N, Huang Y, Li LJ. Synchronous multicentric osteosarcoma involving mandible and maxillas. *Int J Oral Maxillofac Implants*. 2011 Apr;40(4):446-9. <https://doi.org/10.1016/j.ijom.2010.11.003>
3. MacDonald D. The most frequent and/or important lesions that affect the face and the jaws. *Oral Radiol*. 2020 Jan;36(1):1-17. <https://doi.org/10.1007/s11282-019-00367-4>
4. Behere R, Lele S. Synchronous osteosarcoma of mandible. *Oral Surg Oral Med Oral Pathol Oral Radiol Endod*. 2009 May;107(5):e45-9. <https://doi.org/10.1016/j.tripleo.2009.01.035>
5. Fenerty S, Shaw W, Verma R, Syed AB, Kuklani R, Yang J, et al. Florid cemento-osseous dysplasia: review of an uncommon fibro-osseous lesion of the jaw with important clinical implications. *Skeletal Radiol*. 2017 May;46(5):581-90. <https://doi.org/10.1007/s00256-017-2590-0>
6. Consolaro A, Paschoal SR, Ponce JB, Miranda DA. Florid cemento-osseous dysplasia: a contraindication to orthodontic treatment in compromised areas. *Dental Press J Orthod*. 2018 May-Jun;23(3):26-34. <https://doi.org/10.1590/2177-6709.23.3.026-034.ojn>
7. MacDonald-Jankowski DS. Florid cemento-osseous dysplasia: a systematic review. *Dentomaxillofac Radiol*. 2003 May;32(3):141-9. <https://doi.org/10.1259/dmfr/32988764>
8. Pereira DL, Pires FR, Lopes MA, Carlos R, Wright JM, Patel P, et al. Clinical, demographic, and radiographic analysis of 82 patients affected by florid osseous dysplasia: an international collaborative study. *Oral Surg Oral Med Oral Pathol Oral Radiol*. 2016 Aug;122(2):250-7. <https://doi.org/10.1016/j.oooo.2016.04.013>
9. Kato CN, Barra SG, Amaral TM, Silva TA, Abreu LG, Brasileiro CB, et al. Cone-beam computed tomography analysis of cemento-osseous dysplasia-induced changes in adjacent structures in a Brazilian population. *Clin Oral Investig*. 2020 Aug;24(8):2899-908. <https://doi.org/10.1007/s00784-019-03154-x>
10. Tayfur M, Tayfur EK, Balcı MG, Deger AN, Cimen FK, Daltaban F. Bilateral synchronous ossifying fibromas of the mandible: a case report. *Int J Clin Exp Pathol*. 2015 May;8(5):5844-7.
11. Tyagi A, Chaudhary S, Gupta V. Ipsilateral maxillo-mandibular ossifying fibroma. *J Maxillofac Oral Surg*. 2015 Mar;14(S1 Suppl 1):127-32. <https://doi.org/10.1007/s12663-012-0366-6>
12. Akcam T, Altug HA, Karakoc O, Sencimen M, Ozkan A, Bayar GR, et al. Synchronous ossifying fibromas of the jaws: a review. *Oral Surg Oral Med Oral Pathol Oral Radiol*. 2012 Nov;114(5 Suppl):S120-5. <https://doi.org/10.1016/j.oooo.2011.08.007>
13. Campolongo MG, Cabras M, Bava L, Arduino PG, Carbone M. Paget's disease of jaw bones as primary manifestation: a case report of a proper diagnosis made by general dentist. *Gerodontology*. 2018 Jun;35(2):147-50. <https://doi.org/10.1111/ger.12328>
14. Smith BJ, Eveson JW. Paget's disease of bone with particular reference to dentistry. *J Oral Pathol*. 1981 Aug;10(4):233-47. <https://doi.org/10.1111/j.1600-0714.1981.tb01270.x>

15. Sobacchi C, Schulz A, Coxon FP, Villa A, Helfrich MH. Osteopetrosis: genetics, treatment and new insights into osteoclast function. *Nat Rev Endocrinol*. 2013 Sep;9(9):522-36. <https://doi.org/10.1038/nrendo.2013.137>
16. Filho AM, Domingos AC, Freitas DQ, Whaites EJ. Osteopetrosis: a review and report of two cases. *Oral Dis*. 2005 Jan;11(1):46-9. <https://doi.org/10.1111/j.1601-0825.2004.01046.x>
17. Wu CC, Econs MJ, DiMeglio LA, Insogna KL, Levine MA, Orchard PJ, et al. Diagnosis and management of osteopetrosis: consensus guidelines from the osteopetrosis working group. *J Clin Endocrinol Metab*. 2017 Sep;102(9):3111-23. <https://doi.org/10.1210/jc.2017-01127>
18. Sundaragiri KS, Saxena S, Sankhla B, Bhargava A. Non syndromic synchronous multiple odontogenic keratocysts in a western Indian population: A series of four cases. *J Clin Exp Dent*. 2018 Aug;10(8):e831-6. <https://doi.org/10.4317/jced.54616>
19. Scully C, Langdon J, Evans J. Marathon of eponyms: 7 Gorlin-Goltz syndrome (Naevoid basal-cell carcinoma syndrome). *Oral Dis*. 2010 Jan;16(1):117-8. <https://doi.org/10.1111/j.1601-0825.2009.01539.x>
20. Cury SE, Cury MD, Cury SE, Pontes FS, Pontes HA, Rodini C, et al. Bilateral dentigerous cyst in a nonsyndromic patient: case report and literature review. *J Dent Child (Chic)*. 2009 Jan-Apr;76(1):92-6.
21. Freitas DQ, Tempest LM, Sicoli E, Lopes-Neto FC. Bilateral dentigerous cysts: review of the literature and report of an unusual case. *Dentomaxillofac Radiol*. 2006 Nov;35(6):464-8. <https://doi.org/10.1259/dmfr/26194891>
22. Ustuner E, Fitoz S, Atasoy C, Erden I, Akyar S. Bilateral maxillary dentigerous cysts: a case report. *Oral Surg Oral Med Oral Pathol Oral Radiol Endod*. 2003 May;95(5):632-5. <https://doi.org/10.1067/moe.2003.123>
23. Chrcanovic BR, Guimaraes LM, Gomes CC, Gomez RS. Cherubism: a systematic literature review of clinical and molecular aspects. *Int J Oral Maxillofac Surg*. 2021 Jan;50(1):43-53. <https://doi.org/10.1016/j.ijom.2020.05.021>
24. Pontes FS, Ferreira AC, Kato AM, Pontes HA, Almeida DS, Rodini CO, et al. Aggressive case of cherubism: 17-year follow-up. *Int J Pediatr Otorhinolaryngol*. 2007 May;71(5):831-5. <https://doi.org/10.1016/j.ijporl.2007.01.017>
25. Machado RA, Pontes H, Pires FR, Silveira HM, Bufalino A, Carlos R, et al. Clinical and genetic analysis of patients with cherubism. *Oral Dis*. 2017 Nov;23(8):1109-15. <https://doi.org/10.1111/odi.12705>
26. Brabyn P, Capote A, Belloti M, Zylberberg I. Hyperparathyroidism diagnosed due to brown tumors of the jaw: a case report and literature review [Internet]. *J Oral Maxillofac Surg*. 2017 Oct;75(10):2162-9. <https://doi.org/10.1016/j.joms.2017.03.013>
27. Pontes FS, Lopes MA, Souza LL, Rezende DSM, Santos-Silva AR, Jorge Junior, et al. Oral and maxillofacial manifestations of chronic kidney disease-mineral and bone disorder: a multicenter retrospective study [Internet]. *Oral Surg Oral Med Oral Pathol Oral Radiol*. 2018 Jan;125(1):31-43. <https://doi.org/10.1016/j.oooo.2017.09.011>
28. Antonelli JR, Hottel TL. Oral manifestations of renal osteodystrophy: case report and review of the literature. *Spec Care Dentist*. 2003;23(1):28-34. <https://doi.org/10.1111/j.1754-4505.2003.tb00286.x>
29. Raubenheimer EJ, Noffke CE, Hendrik HD. Recent developments in metabolic bone diseases: a gnathic perspective. *Head Neck Pathol*. 2014 Dec;8(4):475-81. <https://doi.org/10.1007/s12105-014-0580-2>
30. Palla B, Burian E, Fliefel R, Otto S. Systematic review of oral manifestations related to hyperparathyroidism. *Clin Oral Investig*. 2018 Jan;22(1):1-27. <https://doi.org/10.1007/s00784-017-2124-0>
31. An SY, Lee JS, Benavides E, Aminlari A, McDonald NJ, Edwards PC, et al. Multiple simple bone cysts of the jaws: review of the literature and report of three cases [Internet]. *Oral Surg Oral Med Oral Pathol Oral Radiol*. 2014 Jun;117(6):e458-69. <https://doi.org/10.1016/j.oooo.2014.03.004>
32. Chrcanovic BR, Gomez RS. Idiopathic bone cavity of the jaws: an updated analysis of the cases reported in the literature [Internet]. *Int J Oral Maxillofac Implants*. 2019 Jul;48(7):886-94. <https://doi.org/10.1016/j.ijom.2019.02.001>
33. Swei Y, Taguchi A, Nagasaki T, Tanimoto K. Radiographic findings and prognosis of simple bone cysts of the jaws. *Dentomaxillofac Radiol*. 2010 Feb;39(2):65-71. <https://doi.org/10.1259/dmfr/54872008>
34. Neves-Silva R, Fernandes DT, Fonseca FP, Pontes HAR, Brasileiro BF, Santos-Silva AR, et al. Oral manifestations of Langerhans cell histiocytosis: A case series. *Spec Care Dentist*. 2018 Nov;38(6):426-33. <https://doi.org/10.1111/scd.12330>
35. Aristizabal Arboleda P, Sánchez-Romero C, Almeida OP, Flores Alvarado SA, Martínez Pedraza R. Calcifying Odontogenic cyst associated with dentigerous cyst in a 15-year-old girl. *Int J Surg Pathol*. 2018 Dec;26(8):758-65. <https://doi.org/10.1177/1066896918777639>
36. Só BB, Carrard VC, Hildebrand LC, Martins MA, Martins MD. Synchronous calcifying epithelial odontogenic tumor: case report and analysis of the 5 cases in the literature. *Head Neck Pathol*. 2020 Jun;14(2):435-41. <https://doi.org/10.1007/s12105-019-01059-5>
37. Shao Z, Liu B, Zhang W, Chen X. Synchronous occurrence of odontogenic myxoma with multiple keratocystic odontogenic tumors in nevoid basal cell carcinoma syndrome. *J Craniofac Surg*. 2013;24(5):1840-2. <https://doi.org/10.1097/SCS.0b013e318275eb4b>